Journal of Inorganic Biochemistry 249 (2023) 112395

Contents lists available at ScienceDirect

Journal of Inorganic Biochemistry

journal homepage: www.elsevier.com/locate/jinorgbio

Exploring the impact of mutation and post-translational modification on α-Synuclein: Insights from molecular dynamics simulations with and without copper

Loizos Savva, James A. Platts *

School of Chemistry, Cardiff University, Park Place, Cardiff CF10 3AT, UK

ARTICLE INFO

Keywords:
Parkinson's disease
Synuclein
Copper
Molecular dynamics
PTM
Mutation

ABSTRACT

We report molecular dynamics simulations of two modifications to α-Synuclein, namely A53T mutation and phosphorylation at Ser129, which have been observed in Parkinson's disease patients. Both modifications are close to known metal binding sites, so as well as each modified peptide we also study Cu(II) bound to N-terminal and C-terminal residues. We show that A53T is predicted to cause increased β-sheet content of the peptide, with a persistent β-hairpin between residues 35–55 particularly notable. Phosphorylation has less effect on secondary structure but is predicted to significantly increase the size of the peptide, especially when bound to Cu(II), which is ascribed to reduced interaction of C-terminal sequence with central non-amyloid component. In addition, estimate of binding free energy to Cu(II) indicates A53T has little effect on metal-ion affinity, whereas phosphorylation markedly enhances the strength of binding. We suggest that the predicted changes in spatial extent and secondary structure of α-Synuclein may have implications for aggregation into Lewy bodies.

1. Introduction

Parkinson's disease (PD) is one of the most prevalent neurodegenerative diseases, characterised by dopamine depletion from neuronal loss in the midbrain. α-Synuclein (αS) is a 140-residue intrinsically disordered protein primarily found in presynaptic terminals of neurons. It has long been implicated with the development of the disease, through its accumulation in Lewy bodies and other pathological aggregates [1]. The protein can be segmented in three main regions (Fig. 1): the N-terminal (M1-K60), identified as the site for membrane and ion interaction; the non-Amyloid-β component (NAC, E61-V95), characterised by its hydrophobic nature and contribution to peptide aggregation; and the C-terminal (K96-A140), which is highly populated by acidic residues and has too been found to bind with metal ions [2,3]. Understanding the factors that influence αS aggregation is crucial for unravelling the underlying mechanisms of PD and developing potential therapeutic strategies.

In the present work, changes to the wild-type (WT) form, which have been prominently associated with the onset of PD are examined. These include the first point mutation flagged in the early discovery of the peptide's association with PD, A53T [4], and the post-translational modification (PTM) reported to be present in 90% of diseased brains, phosphorylation at Ser129 (pS129) [5–7]. Considering the documented effect of copper ion binding to αS [8,9], the work presented here follows previous assessments on the effects of Cu(II) on the WT-αS, published by our group [10]. The metal ion-binding sites in αS, were maintained the same as the ones described in the unaltered form of the protein, between residues M_1DVFMKGLS$_9$, V$_{48}$AHGV$_{52}$ and D$_{119}$PDNEA$_{124}$ [11–14], with the two N-terminal sites forming a macro-chelate, centred on the metal ion; resulting in interactions with M1, D2 and H50, in the N-terminal and D119, D121, N122 and E123, in the C-terminal [10,12,15]. Metal ion coordination at the N-terminus has also been proposed to occur through coordination with M1, D2 and H_2O, and V49, H50 and H_2O (Fig. 2) [16,17].

Despite the high expression of pS129 in patients with PD, as opposed to the 4% occurrence in normal brains, studies on the effect of this form of αS in its ability to aggregate still have not settled on a definite conclusion. In spite of some reports suggesting the promotion of fibrillation upon phosphorylation at Ser129 [5,18,19], other studies argue the phosphorylated form may be an outcome of the disease itself, as a result of proteolysis impairment acting as a signal for degradation [20,21], with no correlation to its ability to form fibrils, or in certain cases inhibiting their expression altogether [20–22]. This potentially protective role is of great interest when considering the pathobiology of

* Corresponding author.
E-mail address: platts@cardiff.ac.uk (J.A. Platts).

https://doi.org/10.1016/j.jinorgbio.2023.112395
Received 16 August 2023; Received in revised form 19 September 2023; Accepted 4 October 2023
Available online 5 October 2023

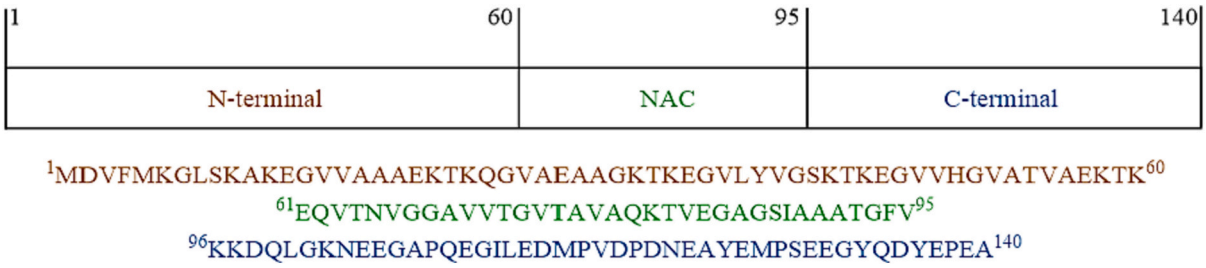

Fig. 1. Residues in the three main regions of α-Synuclein.

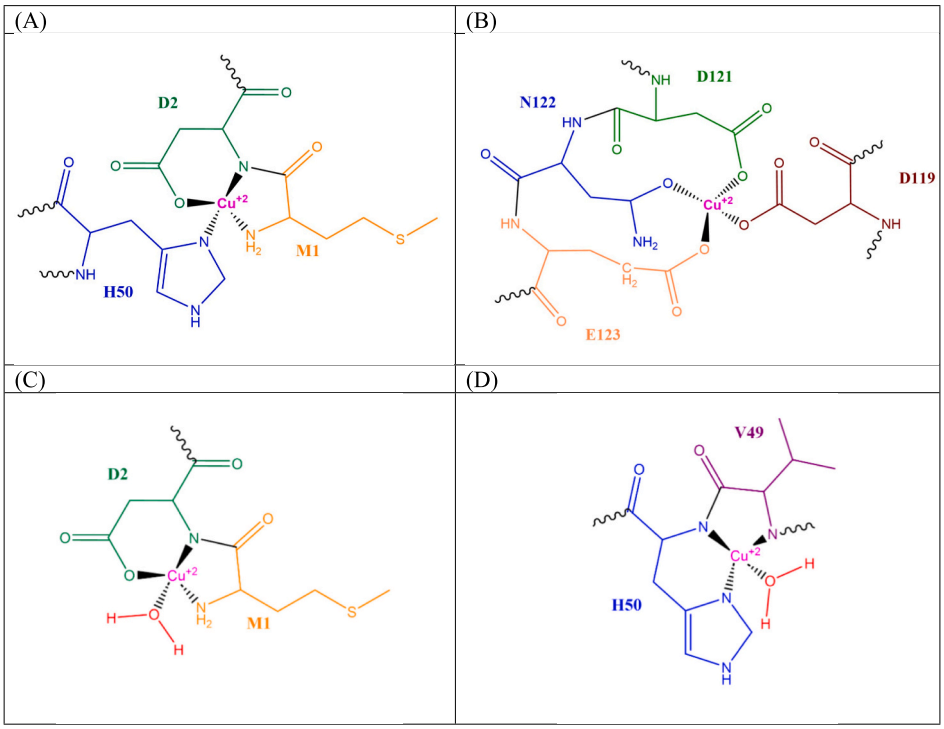

Fig. 2. The four binding sites described in Cu(II) binding with α-Synuclein.

Table 1
Secondary structure content in the three main regions of αS, in its Cu(II)-bound and unbound forms.

Region	β character (%)	α character (%)	Other (%)
Free-αS (WT) [10]			
N-terminal	2.12	16.30	81.58
NAC	6.84	14.56	78.61
C-terminal	0.26	18.05	81.69
Free-αS (A53T)			
N-terminal	1.14	15.32	83.54
NAC	3.18	16.19	80.63
C-terminal	0.14	15.95	83.91
Cu(II)-αS (WT) [10]			
N-terminal	2.45	9.73	87.82
NAC	5.10	14.73	80.18
C-terminal	0.26	14.30	85.44
Cu(II)-αS (A53T)			
N-terminal	2.83	11.45	85.72
NAC	4.86	16.08	79.06
C-terminal	0.15	12.90	86.95

this disease, as it could provide new insights into its development and progression pave the way for novel therapeutic strategies. Given the high prevalence of this particular PTM in Lewy bodies of PD-patients, it is a significant pathological biomarker for misfolded and aggregated αS [7,24]. Notwithstanding the disagreement of studies on the impact of pS129 on the aggregation capacities of αS, it has been shown that oxidative stress induces phosphorylation at S129 [23]. Recognizing the effect of copper coordination to αS, catalysing the production of reactive oxidative species (ROS) [25], as well as experimental evidence suggesting an increase in the binding affinity of divalent metal ions upon phosphorylation of αS [7,26], the Cu(II)-bound pS129-αS was also simulated. Experimental studies on the copper-bound pS129-αS report higher binding affinity in the C-terminal binding site [11,27,28].

Thus far, eight natural point mutations have been identified in the Synuclein Alpha (SNCA) gene [29], with the aggregation process shown to accelerate through at least five of those mutations. The A53T mutation is one of the most common genetic mutations associated with familial forms of PD, and it has been shown to increase the formation of protofibrilar intermediates [30,31]. In particular, this substitution has been described to decrease the enthalpic barrier for nucleation, effectively increasing the formation of nuclei, which are the seeds for fibril growth [32,33]. As a result of the faster kinetics of fibrillation, patients with the A53T mutation have been associated with an earlier age of onset, along with a reported faster progression of PD. [34] This point mutation was first found to exist in familial-PD patients of Greek and Italian descent [4,35]; while later it was also characterised in patients from Sweden [36] and Korea [37]. Several groups have already ventured into identifying changes in the structure and dynamics of the

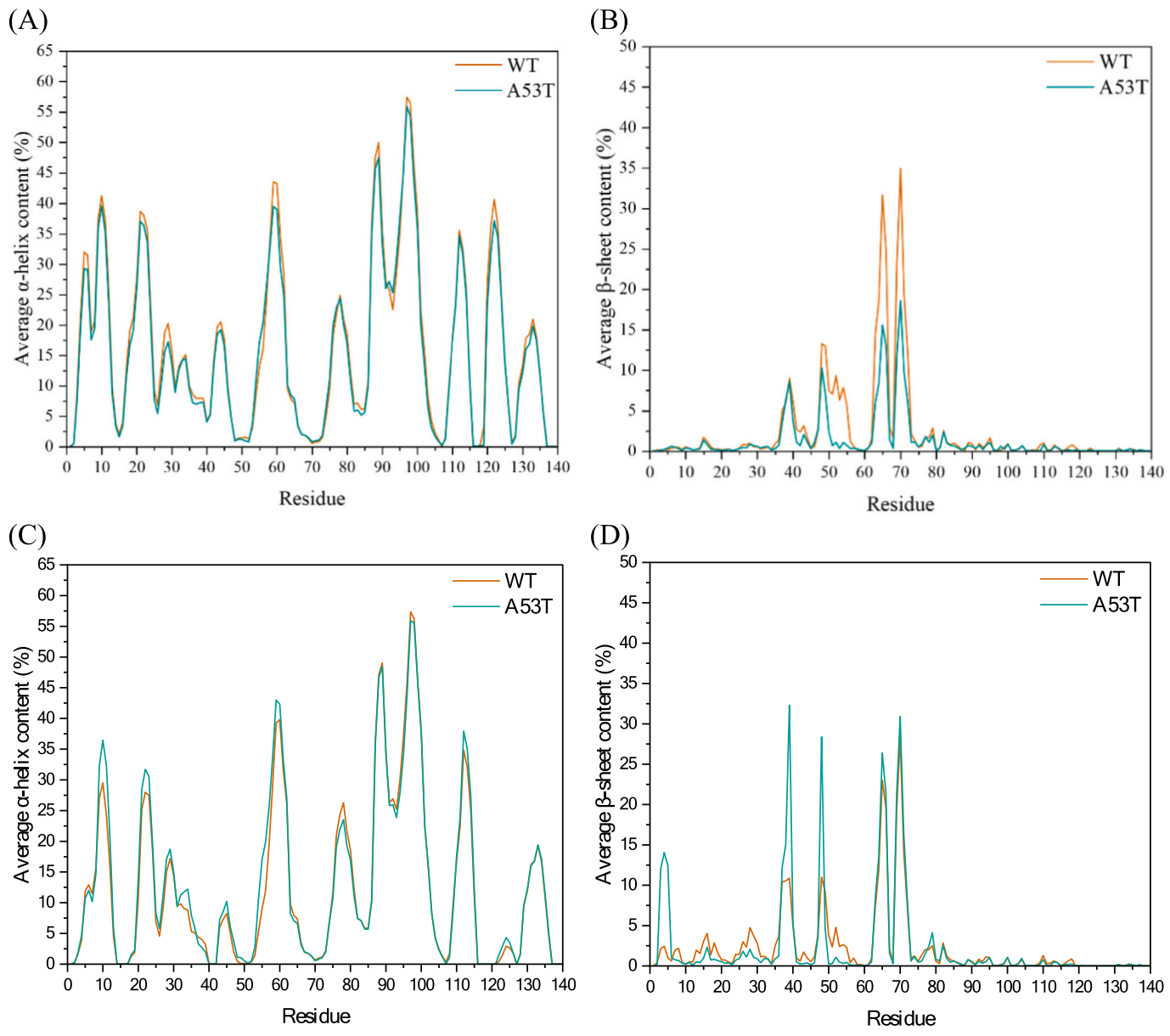

Fig. 3. Average secondary characteristics of residues from the wild-type [10] and mutated (A-B) metal-free and (C—D) metal bound α-Synuclein.

protein, as a result of this mutation [38,39]. The novelty here is in the interplay between metal binding and the A53T mutation, and the effects these could have on the mechanisms underlying PD pathogenesis. In this context, it is notable that both modifications are in close proximity to metal binding residues, A53T with H50 and pS129 with D119-E123.

By elucidating the structural and dynamic effects of Cu(II) binding to the A53T form of αS, we aim to shed light on the mechanisms underlying the enhanced aggregation propensity of this variant. Additionally, the work here provides valuable insights into the interplay between metal ions and disease-associated mutations in αS, which could have implications for the development of novel therapeutic strategies targeting PD and related neurodegenerative diseases.

2. Computational methods

The two chains [αS (A53T) and αS (pS129)] examined here were modelled in their extended conformation in DommiMOE [40], with the ligand-field molecular mechanics (LFMM) force field used for an initial minimisation of the systems, both with and without Cu(II). The MCPB.py [41] package was used to obtain updated parameters for the metal ions and the coordinating atoms, after performing QM calculations on fragments of the binding sites through Gaussian09 [42], using B3LYP/6-31G(d) [43]. For the molecular dynamics simulations the ff03ws force field [44], and Onufriev, Bashford, Case (OBC) modification to the generalised Born (GB) model [45–47], were used to parameterise the systems and perform the simulations using the AMBER16 package [48]. This combination of forcefield and solvent model was extensively tested against secondary structure, radius of gyration and chemical shift in previous work from our group [49]. Parameters for the pS129 residue were obtained from the phosaa10 force field [50,51]. For all simulations, three replicates of 100 ns conventional MD were performed to equilibrate the systems and obtain average potential energies. These were used to extend each of the runs using accelerated MD, by applying a bias on the potential energy of the systems, permitting the exploration of the extended conformational space. Each run was extended by an additional 600 ns aMD, at a 2 fs timestep, resulting in 2.1 μs total simulation time for each system under study. All the simulations were performed in the NVT ensemble, using the Langevin thermostat, at 310 K [52]. The SHAKE algorithm was also used, to impose holonomic restraints on bonds to hydrogen. This parameterisation protocol follows

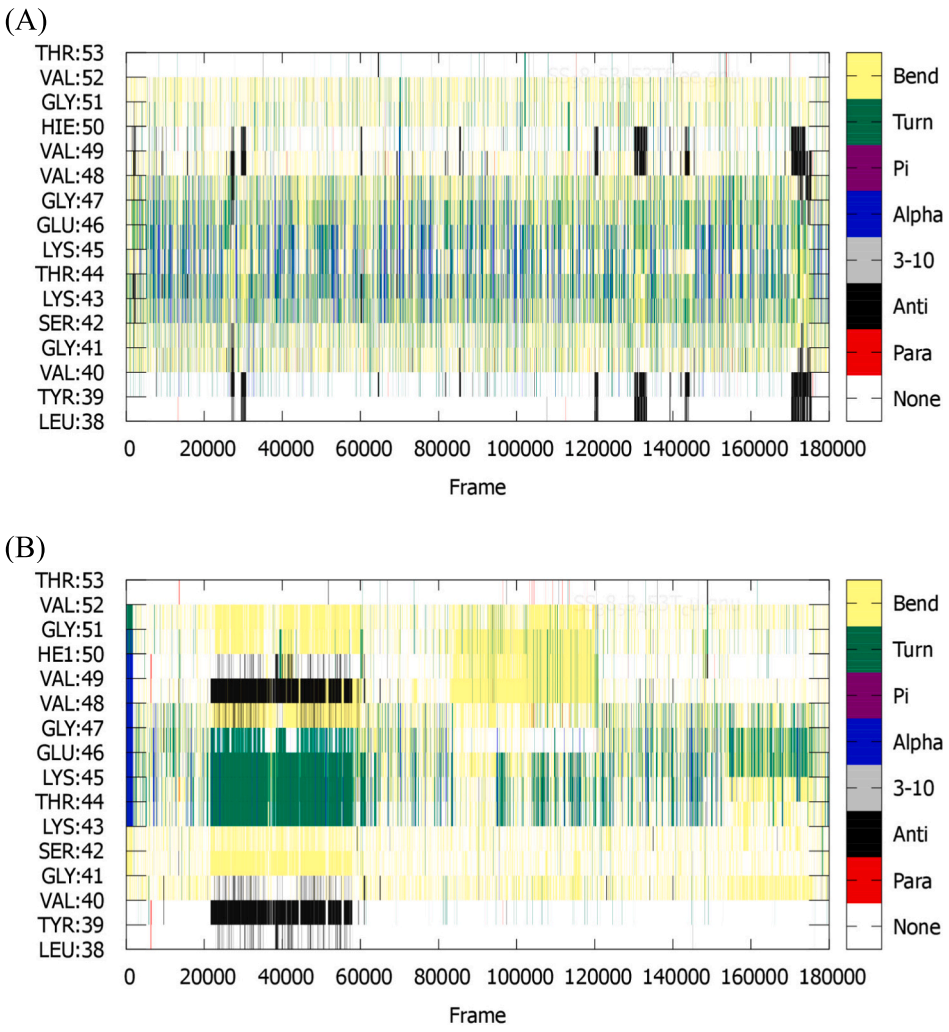

Fig. 4. Evolution of secondary structural elements of each of the residues (L38-A53) in the primary hairpin region from the (A) metal-free and (B) copper-bound A53T-mutated systems.

Table 2
Radius of gyration from the WT[10] and A53T forms of α-Synuclein, with and without Cu(II).

System	Avg. R_g (Å)	SD (Å)	Max. (Å)	Min. (Å)
Free-αS (WT) [10]	44.26	4.58	61.50	28.07
Free-αS (A53T)	50.96	8.94	75.12	29.02
Cu(II)-αS (WT) [10]	34.94	4.06	62.34	21.93
Cu(II)-αS (A53T)	46.83	4.99	64.31	31.63

Table 3
The two most populated clusters from the trajectories of the WT and A53T-mutated systems.

Cluster #	Frames in cluster (out of total 180,000)	Avg. R_g (Å)	SD (Å)
Free-αS (WT) [10]			
1	31.1%	44.91	3.27
2	0.5%	42.19	2.60
Free-αS (A53T)			
1	6.8%	64.61	2.70
2	4.2%	52.10	3.76
Cu(II)-αS (WT) [10]			
1	7.6%	38.15	3.36
2	3.4%	38.31	2.65
Cu(II)-αS (A53T)			
1	2.6%	44.81	3.13
2	2.1%	44.66	4.48

our earlier work on the wild-type (WT) system [10,49], so alterations induced by modification of that form can more easily be identified.

The binding affinity of the metal ion to fragments of the binding sites was also measured, through relaxed potential energy scanning of different distances between the metal ion and one of the coordinating atoms in the sidechain of ligating residues, using GFN2-xTB [53]. The macro-chelate could not be assessed owing to the size of the system and the lack of control on the direction for the increasing distance, that leaves the copper ion interacting with residues along the whole peptide. Instead, a 7-residue fragment (G47-[A/T]53) of the near-range binding site involving V49-H50-H_2O, also described in the literature [16], was modelled as a way of estimating the energy change one can expect from the A53T mutation. For the pS129 system, changes in the C-terminal binding affinity were assessed on the V118-E130 fragment of the protein. Potential energy difference between bound and unbound states was corrected for zero point energy (ZPE), enthalpy and entropy effects, as an approximation for the missing entropic term, whereby G = E + pV + ZPE-TS, with G = Gibbs free energy, and E = electronic energy [54].

The analysis of the trajectories was performed using the cpptraj [55] tool, acquiring data on secondary structure, root mean square fluctuation (RMSF), hydrogen bonding (for distance between donor and

Table 4
Newly formed or broken hydrogen bonds due to A53T mutation (maintained for >10% of the simulations). Brackets have been added to the instances where residues form an additional hydrogen bond through different atoms.

System	Acceptor	Donor	Retention (%)
New Hydrogen Bonds			
Free-αS	Glu61	Val70	10.3
Cu(II)-αS	Glu46	Met1	24.2
	Glu46	Val49	19.4
	Glu46	His50	13.3
	Gly47	Val40	11.7
	Glu46	Val48	11.6
Broken Hydrogen Bonds			
Free-αS	All broken hydrogen bonds exist for <10%		
Cu(II)-αS	Glu35	Val49	28.2
	Glu35	Met1	27.4
	Glu35	His50	21.2
	Glu13	Met1	12.8 (11.0)
	Glu13	His50	11.8 (10.4)
	Glu13	Val52	11.5

acceptor heavy atoms <3.0 Å, and > 5% persistency in the total frames of the MD runs) and radius of gyration (R_g). Data reported is over all aMD simulation (1.8 μs), with first 100 ns of conventional MD taken as equilibration. Clusters were produced using principal component analysis (PCA) of the backbone C's (Cα), through the carma package [56].

3. Results and discussion

3.1. A53T mutation

Evidence on the differences between the wild-type and A53T forms of α-Synuclein have already been published in the literature, both from experimental and computational assessments on the systems [38,57]. Here, we focus on the novelties our study proposes, which come with the introduction of Cu(II)-binding to αS. The possible increase in aggregation from the A53T mutation has been described in the past by an annealing MD study, where no change in the characteristics between the wild-type and mutated forms of the free-monomer was reported [58]. Previous MD simulations on the copper-free wild-type and mutated protein suggest increase in β-strand content in all three regions of the protein, most notably the N-terminal, as a result of the A53T mutation [38]. This increase in the strand content has also been described in a Fourier-transform infrared (FTIR) spectroscopy study, where the section encompassing residues V40-K60 was characterised by an increased presence of β-strand, with a corresponding decrease in the helical content in that same region [57].

Our data (Table 1) indicate very little change in overall secondary structure between WT and mutated peptide without copper, while Cu(II) binding reduces helical content in the N-terminus in both cases. Fig. 3 provides more resolution at per-residue level, showing that the α-helical characteristics remain relatively unchanged between the WT and mutated forms, with the majority of changes observed in the β-character. Considering the involvement of residues L38-A(T)53 in the formation of a stable β-hairpin structure, here we find a significant increase in the strand inclination of that region in the metal-bound peptide. In particular, the mean β-sheet occupancies of residues Tyr39 and Val48, increase from 10.9% and 11.0% in the WT-form, to 32.3% and 28.4% in the A53T-form. The aromaticity present at Tyr39, was recently suggested to be of vital importance to the aggregation of αS [59]. This change was found to result in the maintenance of the β-hairpin for 40,000 frames (67% of a single aMD run), as shown Fig. 4. This, along with the expected conformational assembly of the multi-chain α-Synuclein, with Cu(II) bridging two chains in opposite directions, resulting in inter-chain interactions in this region, possibly makes this system very susceptible to co-assembly.

The A53T mutation introduced a significant increase in the R_g values for both the metal-free and metal-bound systems, as shown in Table 2; much more pronounced in the latter, exhibiting double the size expansion seen in the metal-free system. Nevertheless, considering the conformational space explored in each case, the copper-bound system samples structures with an R_g as low as 29 Å and as high as 75 Å, with a standard deviation (SD) of 9 Å, as opposed to the metal-bound system, where the SD is more in-line with the sampling range seen in the WT-forms, at 5 Å. This overall increase in the expansion of the peptide, is in line with another MD study on the mutated system, where an average difference of 6 Å was reported, between the WT and A53T forms [39].

This increase in the size of the monomer, could suggest the exposure of the central hydrophobic region to inter-chain interactions. This could also be a result of the greater range of chain sizes sampled – also seen from the relatively low-populated clusters of the two systems, Table 3. The two most populated clusters from each system, appear to support the great increase in the appearance of extended conformations, suggestive of a predominantly unfolded ensemble of structures, Fig. S2.

This increase in the size of the copper-bound peptide, in particular, is also reflected by a reorganisation of hydrogen bonding in the region surrounding the N-terminal macro-chelate (Table 4). There, long-range interactions between the coordinating residues and Glu35/Glu13, have now been replaced with hydrogen bonds predominantly with Glu46 – resulting in a less constrained area surrounding the macro-chelate. The effects of this rearrangement of interactions is illustrated in the increased distances observed in the contact map of Cα (Fig. 5) and RMSF (Fig. S1).

The binding free energy of the metal ion to the G47-T53 site

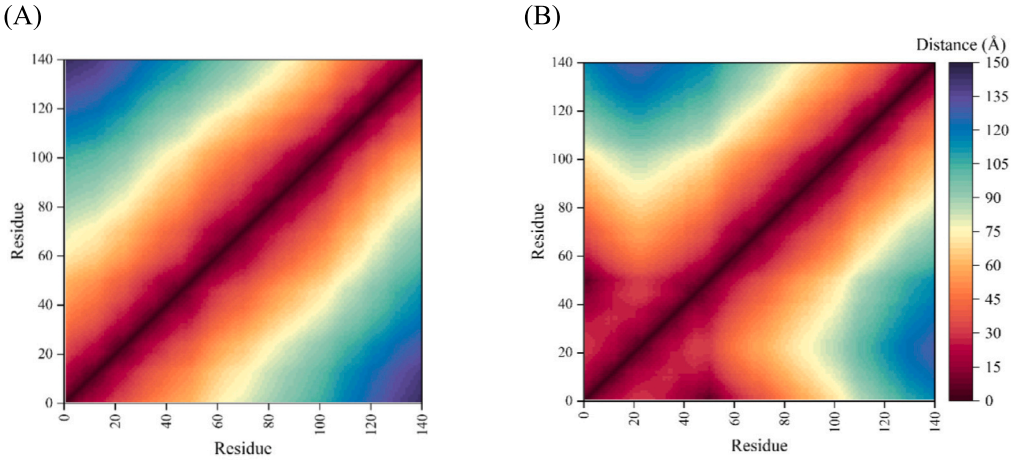

Fig. 5. Contact maps of the distance between the backbone-C in the (A) metal-free and (B) Cu(II)-bound A53T peptides.

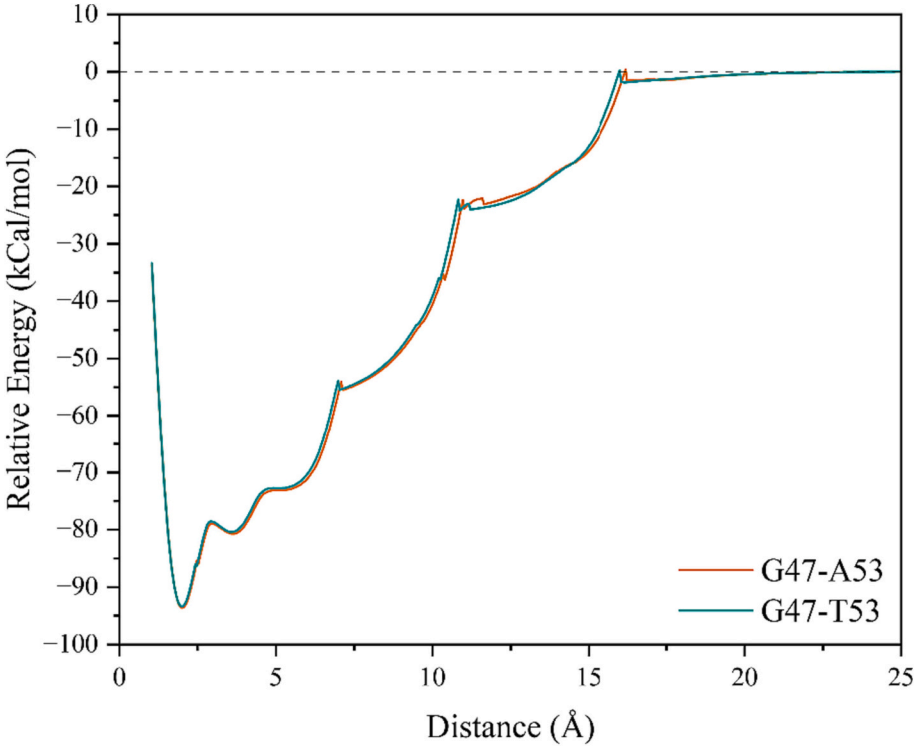

Fig. 6. Relative binding energy of Cu(II) to fragments G47-A53 (WT) and G47-T53 (A53T). The distance is defined between the metal ion and Nδ from the imidazole ring of H50.

Table 5
Radius of gyration from the WT[10] and pS129 forms of α-Synuclein, with and without Cu(II).

System	Avg. R_g (Å)	SD (Å)	Max. (Å)	Min. (Å)
Free-αS (WT) [10]	44.26	4.58	61.50	28.07
Free-αS (pS129)	49.24	8.00	71.39	28.43
Cu(II)-αS (WT) [10]	34.94	4.06	62.34	21.93
Cu(II)-αS (pS129)	44.49	5.75	65.38	27.17

presented only very small change in the energy value from the metal ion in the WT form (G47-A53), as shown in Fig. 6. The binding energy decreased from −85.39 kcal/mol to −85.58 kcal/mol in G47-T53. This could be due to the lack of interactions with residue A(T)53, seeing as it is the last residue in the fragment, along with the minimal effect on the distanced residues from the addition of a methyl and a hydroxyl group by the substitution of Ala with Thr. Whatever the cause, the mutation does not seem to affect the binding of the metal ion to H50. The energy values presented here, deviate from experimentally-expected values by quite a significant degree, given the N-terminal binding energies have been described in the range of −7.5 to −12.5 kcal/mol [16,60]. We attribute this difference in the missing deprotonation energies of the two backbone N, upon coordination of the metal ion. An attempt was made at obtaining the deprotonation energy, using QM optimisation calculations in Gaussian09 (B3LYP/6-31G(d,p)+), on the protonated and deprotonated 3-residue V48-H50 system, and using a solvated proton free energy of −273.07 kcal/mol, from a previous QM study, using the same functional [61]. The deprotonation free energy obtained from these calculations was +67.19 kcal/mol, increasing the binding free energies within reasonable agreement to experiment, to −18.20 kcal/mol and − 18.39 kcal/mol, for G47-A53 and G47-T53. This is by no means an extensive assessment of the system, but it is evidence of the small effect of A53T mutation on the binding energies.

Overall, the findings presented here revealed a significant increase in the R_g values of the mutated systems, especially in the presence of copper ions. The contact maps and RMSF presented increased distances between the residues, as well as higher fluctuations in the N-terminal of the mutated systems. The greater expression of transient β-hairpin structures in the copper-bound mutated peptide, could suggest a greater aggregation propensity of this system, especially considering the involvement of this region in inter-chain interactions.

3.2. *pS129 modification*

Experimental observations on phosphorylated αS system have proposed parallels between the aggregation capabilities of the WT-αS and its pS129 modification, with evidence suggesting fibril formation is not affected by phosphorylation at S129 [20–22]. From what has been reported in the literature, however, phosphorylation appears to increase the binding affinity of the C-terminal to divalent metal ions [7,26]. The distribution of R_g in the metal-free phosphorylated system, Table 5, exhibits similar characteristics to the mutated system, seen above, where the range of conformations sampled is much broader than in the WT-form. Overall, an increase in the expansion of the peptide is seen here, with the greatest change from the WT-form found in the copper-coordinated system, with a *ca.* 10 Å increase in the R_g. In fact, the changes observed in the average R_g here, are in line with those observed in the A53T system, only differing by 1–2 Å. Before exploring further what could constitute the reason for this increase in the size of the systems, we will first consider the changes in the secondary structure characteristics.

Below, the secondary structure distribution of the WT and pS129 systems is shown, Fig. 7. The majority of the characteristics here are similar, except for a decrease in the β-sheet content from 2.5% and 2.2% in the metal-free and Cu(II)-bound WT-form, to 1.5% in the pS129-form. This drop in the metal-free system comes from the NAC region, similarly to the A53T system. This is not the case, however, for Cu(II)-αS where the decrease is from the N-terminal of the peptide, going from 2.5% in the WT-form to 0.6% in pS129-αS, Table 6. This overall reduction in the β-content of the systems, could hint towards a decrease in the

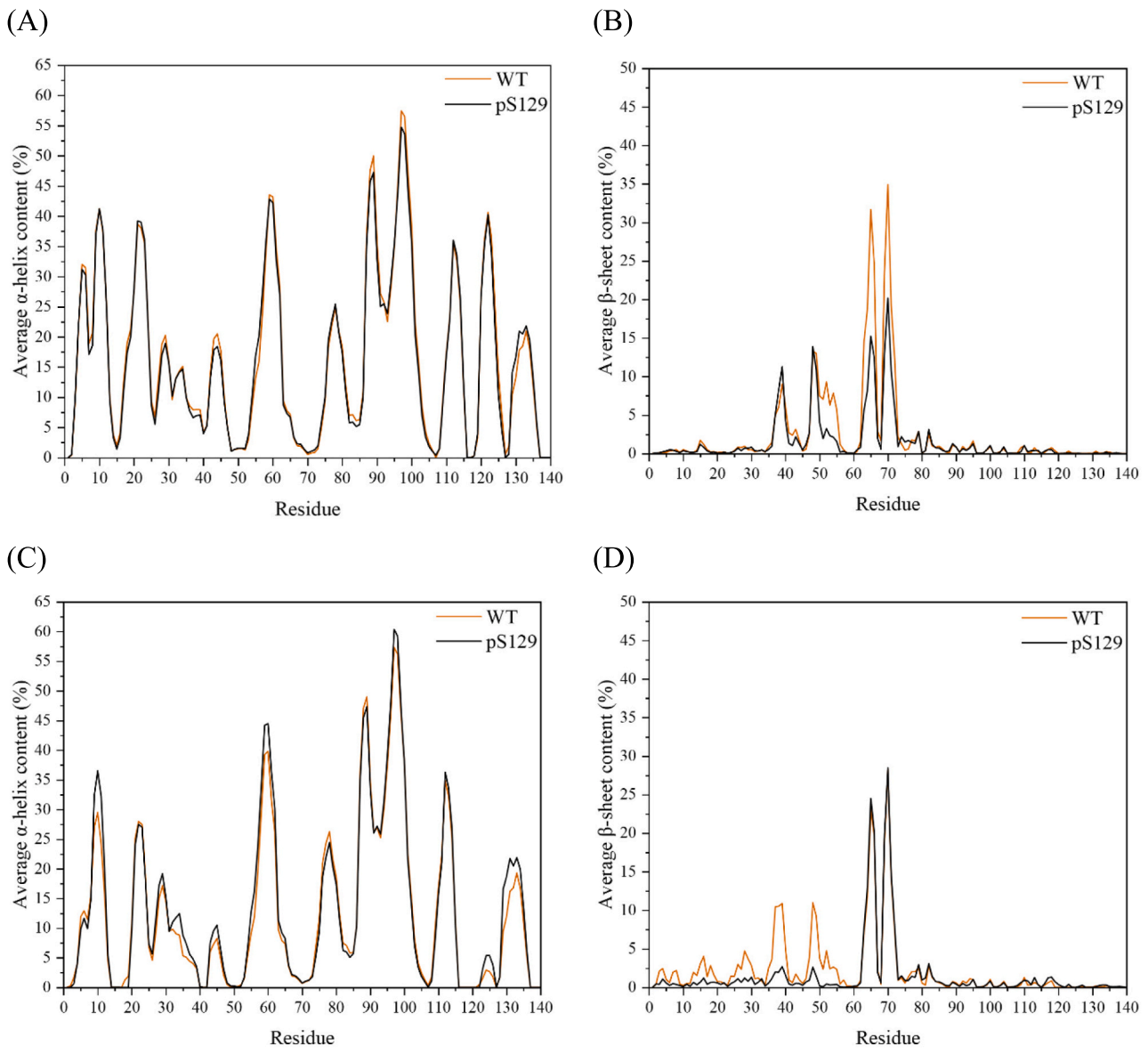

Fig. 7. Average secondary characteristics of residues from the wild-type [10] and pS129-modified (A-B) metal-free and (C—D) metal bound α-Synuclein.

Table 6
Secondary structure content in the three main regions of αS, in its Cu(II)-bound and unbound forms.

Region	β character (%)	α character (%)	Other (%)
Free-αS (WT) [10]			
N-terminal	2.12	16.30	81.58
NAC	6.84	14.56	78.61
C-terminal	0.26	18.05	81.69
Free-αS (pS129)			
N-terminal	1.54	16.05	82.41
NAC	3.41	16.03	80.56
C-terminal	0.17	16.60	83.23
Cu(II)-αS (WT) [10]			
N-terminal	2.45	9.73	87.82
NAC	5.10	14.73	80.18
C-terminal	0.26	14.30	85.44
Cu(II)-αS (pS129)			
N-terminal	0.65	10.95	88.40
NAC	4.62	16.61	78.77
C-terminal	0.30	13.61	86.09

Table 7
Newly formed or broken hydrogen bonds in the pS129 systems (maintained for >10% of the simulations). Brackets have been added to the instances where residues form an additional hydrogen bond through different atoms.

System	Acceptor	Donor	Retention (%)
New Hydrogen Bonds			
Free-αS	All newly formed hydrogen bonds exist for <10%		
Cu(II)-αS	Asp119	Val118	12.8
	Glu131	Asn122	11.5 (11.3)
Broken Hydrogen Bonds			
Free-αS	All broken hydrogen bonds exist for <10%		
Cu(II)-αS	Glu35	Val49	28.2
	Glu35	Met1	27.4
	Glu35	His50	21.2
	Glu13	Met1	12.8 (11.0)
	Glu13	His50	11.8 (10.4)
	Glu13	Val52	11.5

aggregation propensity of the peptide, as a result of the phosphorylation at S129, restricting the inter-peptide interactions that could form. This is further supported by experimental evidence, using a Thioflavin-T

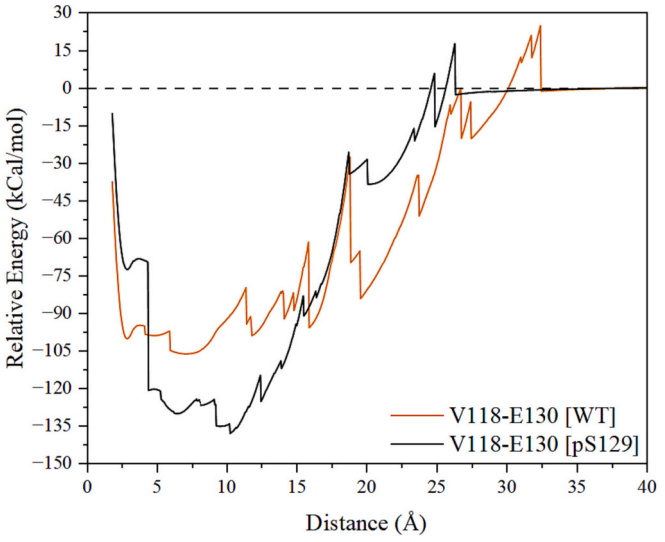

Fig. 8. Relative binding energy of Cu(II) to the C-terminal binding site of the WT and pS129-αS, calculated on the V118-E130 fragment. The distance is defined between the metal ion and O from the carboxyl group of D121.

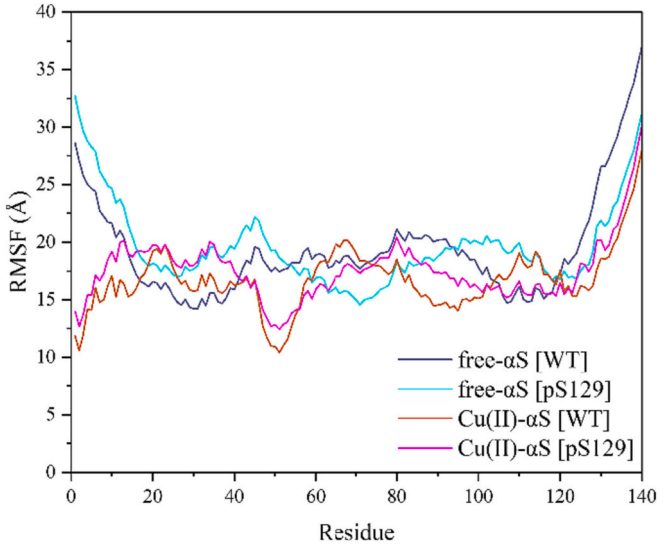

Fig. 9. RMSF of the residues in the metal-free and Cu(II)-bound peptides, in the pS129 system.

fluorescence binding assay, which showed a decrease in the aggregation of the phosphorylated αS [22]. The increased size of the copper-bound protein, appears to be influenced by this drop in the β-character of the N-terminal, as this is the region where the most significant expansion originates, Table S5.

Looking at the newly formed hydrogen bonds, Table 7, their appearance in the C-terminal is rationalised by the 2 Å reduced R_g compared to WT, Table S5, as well as the decreased end-to-end distance of that region, from 60 in the WT to 56 Å in the pS129-αS. The hydrogen bonds that are broken have eased the strain around the Cu(II)-binding site, with the structural geometry now more in line with the bond angles expected in a square planar conformation, Table S3.

The drop in the C-terminal end-to-end distance of the metal-bound system indicates a tendency for the residues in this region to 'envelop' more closely around the metal, suggesting the greater submission of the residues to the electrostatic effects from the metal ion. Further evidence comes from the C-terminal binding energy for each of the systems, which was obtained from semiempirical measurements, after increasing the distance between the metal ion and O from the carboxyl group of D121, in V118-E130. Fig. 8, displays the relative binding energy of the metal ion to this site, where an overall increase in affinity is observed in the pS129 system. The binding free energy here decreases from −107.85 kcal/mol to −131.20 kcal/mol, going from the WT to pS129 system. These results appear to support experimental observations, where a small increase in the binding affinity to the C-terminal is seen, upon phosphorylation of Ser129, from −10.49 kcal/mol to −10.63 kcal/mol [7,26]. The great difference between the binding energies from the semiempirical calculations and the experimental values, was something also observed in the mutated system above; although no further corrections were made to the values calculated from the semiempirical approach here, which are mainly believed to arise from the desolvation of Cu(II) upon coordination with the four carboxylate sidechains. Nevertheless, it is unlikely that these would significantly alter the overall trend in the binding energies and the relative increase in the binding affinity of the metal ion to the C-terminal, which admittedly is expected to be larger than what is observed experimentally.

The RMSF values, Fig. 9, did not present any significant changes in the fluctuation of the residues, going from the WT to the pS129 systems, overall maintaining the same trend, with a maximum difference of *ca.* 6 and 4 Å in the metal-free and Cu(II)-bound systems, respectively. These differences are expressed between residues E130-A140 in the former, and A11-V16 in the latter. In the case of the metal-bound system, the difference comes from an increase in the fluctuations, which appears to be a result of the overall breakage of hydrogen bonds in the N-terminal, Table 7. The decrease in the fluctuations in the metal-free peptide, are in line with the motion seen in the phosphorylated metal-bound system. However, the inherently unstructured nature of the C-terminal of αS, makes it difficult to associate the changes in the fluctuations to a specific structural feature in that region, and could instead be a result of the carrying effect from the less noticeable drop in the motion of residues in the NAC region.

Considering the evidence presented here, phosphorylation of αS at S129 does not alter the conformation and dynamics of the protein in a significant manner to elicit a notable change in fibril formation, with minor reduction in the β-content and overall size of the chains. Nevertheless, an increase in the binding affinity of the C-terminal to Cu(II) is observed, which could potentially lead to stabilisation of the folding structures in that region, also seen by the increase in the amount of helix and strand content.

4. Conclusions

Post translational modifications and mutations to the WT-αS have long been identified as potential factors in the development of PD. Here, the effects of two such modifications, namely the phosphorylation of S129 and A53T mutation, were examined in the context of the metal-free and Cu(II)-bound αS. These two alterations were selected, as their presence has been recorded in diseased brains, raising interest on their effects in the structure and aggregation properties of the protein. In particular, pS129 has been identified as the primary phosphorylation site, exhibited in the majority of patients with PD [7], while the A53T mutation has been linked with familial cases of PD. [4]

Each of the modifications to the WT-αS examined here, introduce their own alterations to the initial state of the system. The most significant of those changes, appear to occur in the A53T Cu(II)-bound system, where the β-hairpin region between residues L38-A(T)53 was found to be maintained for almost the entirety of one of the runs, and *ca.* 22% of all recorded frames, compared to 4% in WT (population of L38-A(T)53 β-hairpin in the metal-free αS, out of all the frames in A53T: 6%; WT: 2%) [10]. Significant contribution to the β-strand content in that region, came from residues Y39 and V48, which almost tripled the persistency of β-characteristics observed in the WT-form. The former residue has been reported to greatly contribute in the aggregation capacities of this

protein [59]. This, along with the expansion of the NAC region, increases the prospect for inter-peptide interactions to form and oligomerisation to occur.

Despite the great expression of the pS129 PTM in patients with PD system, the data presented here suggest a likely decrease in the aggregation capacities of the protein, from a reduced β-sheet content in both the unbound and Cu(II)-bound systems. The C-terminal of the pS129-systems display a reduced size, which has been attributed to an increased affinity for the metal ion in that site, seen from the reduced binding free energy, whereas the peptide as a whole exhibits significantly greater spatial extent when phosphorylated in both metal-free and copper-bound cases.

Credit authors

LS and JAP designed the study; LS carried out simulations and analysis; LS and JAP wrote the manuscript.

Declaration of Competing Interest

We hereby declare that authors have no competing interests, and that this is an exclusive submission to J Inorg Biochem.

Data availability

Data will be made available on request.

Acknowledgements

We acknowledge the role of Advanced Research Computing @ Cardiff (ARCCA) in providing computational resources for simulations.

Appendix A. Supplementary data

Supplementary data to this article can be found online at https://doi.org/10.1016/j.jinorgbio.2023.112395.

References

[1] M. Goedert, R. Jakes, M.G. Spillantini, The Synucleinopathies: twenty years on, J. Parkinsons Dis. 7 (2017) S53–S71.
[2] K. Uéda, H. Fukushima, E. Masliah, Y.U. Xia, A. Iwai, M. Yoshimoto, D.A.C. Otero, J. Kondo, Y. Ihara, T. Saitoh, Molecular cloning of cDNA encoding an unrecognized component of amyloid in Alzheimer disease, Proc. Natl. Acad. Sci. U. S. A. 90 (1993) 11282–11286.
[3] A.D. Stephens, M. Zacharopoulou, R. Moons, G. Fusco, N. Seetaloo, A. Chiki, P. J. Woodhams, I. Mela, H.A. Lashuel, J.J. Phillips, A. De Simone, F. Sobott, G.S. K. Schierle, Extent of N-terminus exposure of monomeric alpha-synuclein determines its aggregation propensity, Nat. Commun. 11 (2020) 2820.
[4] M.H. Polymeropoulos, C. Lavedan, E. Leroy, S.E. Ide, A. Dehejia, A. Dutra, B. Pike, H. Root, J. Rubenstein, R. Boyer, E.S. Stenroos, S. Chandrasekharappa, A. Athanassiadou, T. Papapetropoulos, W.G. Johnson, A.M. Lazzarini, R. C. Duvoisin, G. Di Iorio, L.I. Golbe, R.L. Nussbaum, Mutation in the α-synuclein gene identified in families with Parkinson's disease, Science 276 (1997) 2045–2047.
[5] H. Fujiwara, M. Hasegawa, N. Dohmae, A. Kawashima, E. Masliah, M.S. Goldberg, J. Shen, K. Takio, T. Iwatsubo, A-Synuclein is phosphorylated in Synucleinopathy lesions, Nat. Cell Biol. 4 (2002) 160–164.
[6] J.P. Anderson, D.E. Walker, J.M. Goldstein, R. De Laat, K. Banducci, R. J. Caccavello, R. Barbour, J. Huang, K. Kling, M. Lee, L. Diep, P.S. Keim, X. Shen, T. Chataway, M.G. Schlossmacher, P. Seubert, D. Schenk, S. Sinha, W.P. Gai, T. J. Chilcote, Phosphorylation of Ser-129 is the dominant pathological modification of α-synuclein in familial and sporadic lewy body disease, J. Biol. Chem. 281 (2006) 29739–29752.
[7] A. Oueslati, Implication of alpha-Synuclein phosphorylation at S129 in Synucleinopathies: what have we learned in the last decade? J. Parkinsons Dis. 6 (2016) 39–51.
[8] X. Wang, D. Moualla, J.A. Wright, D.R. Brown, Copper binding regulates intracellular alpha-synuclein localisation, aggregation and toxicity, J. Neurochem. 113 (2010) 704–714.
[9] D.R. Brown, Oligomeric alpha-synuclein and its role in neuronal death, IUBMB Life 62 (2010) 334–339.
[10] L. Savva, J.A. Platts, How cu(II) binding affects structure and dynamics of α-synuclein revealed by molecular dynamics simulations, J. Inorg. Biochem. 239 (2023) 112068.
[11] A. Binolfi, R.M. Rasia, C.W. Bertoncini, M. Ceolin, M. Zweckstetter, C. Griesinger, T.M. Jovin, C.O. Fernández, Interaction of α-synuclein with divalent metal ions reveals key differences: a link between structure, binding specificity and fibrillation enhancement, J. Am. Chem. Soc. 128 (2006) 9893–9901.
[12] R.M. Rasia, C.W. Bertoncini, D. Marsh, W. Hoyer, D. Cherny, M. Zweckstetter, C. Griesinger, T.M. Jovin, C.O. Fernández, Structural characterization of copper(II) binding to α-synuclein: insights into the bioinorganic chemistry of Parkinson's disease, Proc. Natl. Acad. Sci. U. S. A. 102 (2005) 4294–4299.
[13] F. Camponeschi, D. Valensin, I. Tessari, L. Bubacco, S. Dell'Acqua, L. Casella, E. Monzani, E. Gaggelli, G. Valensin, Copper(I)-α-Synuclein interaction: structural description of two independent and competing metal binding sites, Inorg. Chem. 52 (2013) 1358–1367.
[14] S.C. Drew, L.L. Su, C.L.L. Pham, D.J. Tew, C.L. Masters, L.A. Miles, R. Cappai, K. J. Barnham, Cu2+ binding modes of recombinant α-synuclein - insights from EPR spectroscopy, J. Am. Chem. Soc. 130 (2008) 7766–7773.
[15] A. Binolfi, L. Quintanar, C.W. Bertoncini, C. Griesinger, C.O. Fernández, Bioinorganic chemistry of copper coordination to alpha-synuclein: relevance to Parkinson's disease, Coord. Chem. Rev. 256 (2012) 2188–2201.
[16] D. Valensin, F. Camponeschi, M. Luczkowski, M.C. Baratto, M. Remelli, G. Valensin, H. Kozlowski, The role of His-50 of α-synuclein in binding cu(ii): PH dependence, speciation, thermodynamics and structure, Metallomics 3 (2011) 292–302.
[17] A. Villar-Piqué, G. Rossetti, S. Ventura, P. Carloni, C.O. Fernández, T.F. Outeiro, Copper(II) and the pathological H50Q α-synuclein mutant: environment meets genetics, Commun. Integr. Biol. 10 (2017) 1–4.
[18] V.N. Uversky, Neuropathology, biochemistry, and biophysics of α-synuclein aggregation, J. Neurochem. 103 (2007) 17–37.
[19] M.R. Ma, Z.W. Hu, Y.F. Zhao, Y.X. Chen, Y.M. Li, Phosphorylation induces distinct alpha-synuclein strain formation, Sci. Rep. 6 (2016) 1–11.
[20] S. Azeredo da Silveira, B.L. Schneider, C. Cifuentes-Diaz, D. Sage, T. Abbas-Terki, T. Iwatsubo, M. Unser, P. Aebischer, Phosphorylation does not prompt, nor prevent, the formation of -synuclein toxic species in a rat model of Parkinson's disease, Hum. Mol. Genet. 18 (2008) 872–887.
[21] R. Bell, M. Vendruscolo, Modulation of the interactions between α-Synuclein and lipid membranes by post-translational modifications, Front. Neurol. 12 (2021) 1–22.
[22] S.S. Ghanem, N.K. Majbour, N.N. Vaikath, M.T. Ardah, D. Erskine, N.M. Jensen, M. Fayyad, I.P. Sudhakaran, E. Vasili, K. Melachroinou, I.Y. Abdi, I. Poggiolini, P. Santos, A. Dorn, P. Carloni, K. Vekrellis, J. Attems, I. McKeith, T.F. Outeiro, P. H. Jensen, O.M.A. El-Agnaf, α-Synuclein phosphorylation at serine 129 occurs after initial protein deposition and inhibits seeded fibril formation and toxicity, Proc. Natl. Acad. Sci. U. S. A. 119 (2022) e2109617119.
[23] W.W. Smith, R.L. Margolis, X. Li, J.C. Troncoso, M.K. Lee, V.L. Dawson, T. M. Dawson, T. Iwatsubo, C.A. Ross, α-synuclein phosphorylation enhances eosinophilic cytoplasmic inclusion formation in SH-SY5Y cells, J. Neurosci. 25 (2005) 5544–5552.
[24] C. Cariulo, P. Martufi, M. Verani, L. Azzollini, G. Bruni, A. Weiss, S.M. Deguire, H. A. Lashuel, E. Scaricamazza, G.M. Sancesario, T. Schirinzi, N.B. Mercuri, G. Sancesario, A. Caricasole, L. Petricca, Phospho-S129 alpha-Synuclein is present in human plasma but not in cerebrospinal fluid as determined by an ultrasensitive immunoassay, Front. Neurosci. 13 (2019) 1–13.
[25] R. De Ricco, D. Valensin, S. Dell'Acqua, L. Casella, P. Dorlet, P. Faller, C. Hureau, Remote His50 acts as a coordination switch in the high-affinity N-terminal centered copper(II) site of α-Synuclein, Inorg. Chem. 54 (2015) 4744–4751.
[26] Y. Lu, M. Prudent, B. Fauvet, H.A. Lashuel, H.H. Girault, Phosphorylation of α-synuclein at Y125 and S129 alters its metal binding properties: implications for understanding the role of α-synuclein in the pathogenesis of Parkinson's disease and related disorders, ACS Chem. Neurosci. 2 (2011) 667–675.
[27] J.A. Castillo-Gonzalez, M.D.J. Loera-Arias, O. Saucedo-Cardenas, R. Montes-de-Oca-Luna, A. Garcia-Garcia, H. Rodriguez-Rocha, Phosphorylated α -Synuclein-copper complex formation in the pathogenesis of Parkinson's disease, Parkinsons Dis. 2017 (2017) 1–9.
[28] N. González, T. Arcos-López, A. König, L. Quintanar, M. Menacho Márquez, T. F. Outeiro, C.O. Fernández, Effects of alpha-synuclein post-translational modifications on metal binding, J. Neurochem. 150 (2019) 507–521.
[29] L. Gadhe, A. Sakunthala, S. Mukherjee, N. Gahlot, R. Bera, A.S. Sawner, P. Kadu, S. K. Maji, Intermediates of α-synuclein aggregation: implications in Parkinson's disease pathogenesis, Biophys. Chem. 281 (2022) 106736.
[30] H.A. Lashuel, B.M. Petre, J. Wall, M. Simon, R.J. Nowak, T. Walz, P.T. Lansbury, A-Synuclein, especially the Parkinson'S disease-associated mutants, forms pore-like annular and tubular Protofibrils, J. Mol. Biol. 322 (2002) 1089–1102.
[31] N. Bengoa-Vergniory, R.F. Roberts, R. Wade-Martins, J. Alegre-Abarrategui, Alpha-synuclein oligomers: a new hope, Acta Neuropathol. 134 (2017) 819–838.
[32] G.A.P. de Oliveira, J.L. Silva, Alpha-synuclein stepwise aggregation reveals features of an early onset mutation in Parkinson's disease, Commun. Biol. (2023), https://doi.org/10.1038/s42003-019-0598-9.
[33] T. Ohgita, N. Namba, H. Kono, T. Shimanouchi, H. Saito, Mechanisms of enhanced aggregation and fibril formation of Parkinson's disease-related variants of α-synuclein, Sci. Rep. 12 (2022) 1–13.
[34] M. Perni, A. van der Goot, R. Limbocker, T.J. van Ham, F.A. Aprile, C.K. Xu, P. Flagmeier, K. Thijssen, P. Sormanni, G. Fusco, S.W. Chen, P.K. Challa, J. B. Kirkegaard, R.F. Laine, K.Y. Ma, M.B.D. Müller, T. Sinnige, J.R. Kumita, S.I. A. Cohen, R. Seinstra, G.S. Kaminski Schierle, C.F. Kaminski, D. Barbut, A. De

Simone, T.P.J. Knowles, M. Zasloff, E.A.A. Nollen, M. Vendruscolo, C.M. Dobson, Comparative studies in the A30P and A53T α-synuclein *C. elegans* strains to investigate the molecular origins of Parkinson's disease, Front. Cell Dev. Biol. (2023), https://doi.org/10.3389/fcell.2021.552549.

[35] A. Athanassiadou, G. Voutsinas, L. Psiouri, E. Leroy, M.H. Polymeropoulos, A. Ilias, G.M. Maniatis, T. Papapetropoulos, Genetic analysis of families with Parkinson disease that carry the Ala53Thr mutation in the gene encoding α-synudein [1], Am. J. Hum. Genet. 65 (1999) 555–558.

[36] A. Puschmann, O.A. Ross, C. Vilariño-Güell, S.J. Lincoln, J.M. Kachergus, S. A. Cobb, S.G. Lindquist, J.E. Nielsen, Z.K. Wszolek, M. Farrer, H. Widner, D. van Westen, D. Hägerström, K. Markopoulou, B.A. Chase, K. Nilsson, J. Reimer, C. Nilsson, A Swedish family with de novo α-synuclein A53T mutation: evidence for early cortical dysfunction, Parkinsonism Relat. Disord. 15 (2009) 627–632.

[37] C.-S. Ki, E. Stavrou, N. Davanos, W. Lee, E. Chung, J.-Y. Kim, A. Athanassiadou, The Ala53Thr mutation in the α-synuclein gene in a Korean family with Parkinson disease, Clin. Genet. 71 (2007) 471–473.

[38] O. Coskuner, O. Wise-Scira, Structures and free energy landscapes of the A53T mutant-type α-synuclein protein and impact of A53T mutation on the structures of the wild-type α-synuclein protein with dynamics, ACS Chem. Neurosci. 4 (2013) 1101–1113.

[39] V. Losasso, A. Pietropaolo, C. Zannoni, S. Gustincich, P. Carloni, Structural role of compensatory amino acid replacements in the α-synuclein protein, Biochemistry 50 (2011) 6994–7001.

[40] R.J. Deeth, N. Fey, B. Williams-Hubbard, DommiMOE: an implementation of ligand field molecular mechanics in the molecular operating environment, J. Comput. Chem. 26 (2005) 123–130.

[41] P. Li, K.M. Merz, MCPB.py: a python based metal center parameter builder, J. Chem. Inf. Model. 56 (2016) 599–604.

[42] M.J. Frisch, G.W. Trucks, H.B. Schlegel, G.E. Scuseria, M.A. Robb, J.R. Cheeseman, G. Scalmani, V. Barone, B. Mennucci, G.A. Petersson, H. Nakatsuji, M. Caricato, X. Li, H.P. Hratchian, A.F. Izmaylov, J. Bloino, G. Zheng, J.L. Sonnenberg, M. Hada, M. Ehara, K. Toyota, R. Fukuda, J. Hasegawa, M. Ishida, T. Nakajima, Y. Honda, O. Kitao, H. Nakai, T. Vreven, J.A. Montgomery Jr., J.E. Peralta, F. Ogliaro, M. Bearpark, J.J. Heyd, E. Brothers, K.N. Kudin, V.N. Staroverov, R. Kobayashi, J. Normand, K. Raghavachari, A. Rendell, J.C. Burant, S.S. Iyengar, J. Tomasi, M. Cossi, N. Rega, J.M. Millam, M. Klene, J.E. Knox, J.B. Cross, V. Bakken, C. Adamo, J. Jaramillo, R. Gomperts, R.E. Stratmann, O. Yazyev, A.J. Austin, R. Cammi, C. Pomelli, J.W. Ochterski, R.L. Martin, K. Morokuma, V.G. Zakrzewski, G.A. Voth, P. Salvador, J.J. Dannenberg, S. Dapprich, A.D. Daniels, Ö. Farkas, J. B. Foresman, J.V. Ortiz, J. Cioslowski, D.J. Fox, Gaussian 09, Wallingford, CT, 2009.

[43] A.P. Scott, L. Radom, Harmonic vibrational frequencies: an evaluation of Hartree-Fock, Møller-Plesset, quadratic configuration interaction, density functional theory, and semiempirical scale factors, J. Phys. Chem. 100 (1996) 16502–16513.

[44] R.B. Best, W. Zheng, J. Mittal, Balanced protein-water interactions improve properties of disordered proteins and non-specific protein association, J. Chem. Theory Comput. 10 (2014) 5113–5124.

[45] G.D. Hawkins, C.J. Cramer, D.G. Truhlar, Pairwise solute descreening of solute charges from a dielectric medium, Chem. Phys. Lett. 246 (1995) 122–129.

[46] G.D. Hawkins, C.J. Cramer, D.G. Truhlar, Parametrized models of aqueous free energies of solvation based on pairwise Descreening of solute atomic charges from a dielectric medium, J. Phys. Chem. 100 (1996) 19824–19839.

[47] A. Onufriev, D. Bashford, D.A. Case, Modification of the generalized born model suitable for macromolecules, J. Phys. Chem. B 104 (2000) 3712–3720.

[48] D.A. Case, R.M. Betz, D.S. Cerutti, T.E. Cheatham, T.A. Darden, R.E. Duke, T. J. Giese, H. Gohlke, A.W. Goetz, N. Homeyer, S. Izadi, P. Janowski, J. Kaus, A. Kovalenko, T.S. Lee, S. LeGrand, P. Li, C. Lin, T. Luchko, R. Luo, B. Madej, D. Mermelstein, K.M. Merz, G. Monard, H. Nguyen, H.T. Nguyen, I. Omelyan, A. Onufriev, D.R. Roe, A. Roitberg, C. Sagui, C.L. Simmerling, W.M. Botello-Smith, J. Swails, R.C. Walker, J. Wang, R.M. Wolf, X. Wu, L. Xiao, P.A. Kollman, AMBER 2016, San Francisco, 2016.

[49] L. Savva, J.A. Platts, Evaluation of implicit solvent models in molecular dynamics simulation of α-Synuclein, J. Biomol. Struct. Dyn. 41 (2022) 1–16.

[50] N. Homeyer, A.H.C. Horn, H. Lanig, H. Sticht, AMBER force-field parameters for phosphorylated amino acids in different protonation states: phosphoserine, phosphothreonine, phosphotyrosine, and phosphohistidine, J. Mol. Model. 12 (2006) 281–289.

[51] T. Steinbrecher, J. Latzer, D.A. Case, Revised AMBER parameters for bioorganic phosphates, J. Chem. Theory Comput. 8 (2012) 4405–4412.

[52] J.A. Izaguirre, D.P. Catarello, J.M. Wozniak, R.D. Skeel, Langevin stabilization of molecular dynamics, J. Chem. Phys. 114 (2001) 2090–2098.

[53] C. Bannwarth, S. Ehlert, S. Grimme, GFN2-xTB - an accurate and broadly parametrized self-consistent tight-binding quantum chemical method with multipole electrostatics and density-dependent dispersion contributions, J. Chem. Theory Comput. 15 (2019) 1652–1671.

[54] J.P. Menzel, M. Kloppenburg, J. Belić, H.J.M. de Groot, L. Visscher, F. Buda, Efficient workflow for the investigation of the catalytic cycle of water oxidation catalysts: combining GFN-xTB and density functional theory, J. Comput. Chem. 42 (2021) 1885–1894.

[55] D.R. Roe, T.E. Cheatham, PTRAJ and CPPTRAJ: software for processing and analysis of molecular dynamics trajectory data, J. Chem. Theory Comput. 9 (2013) 3084–3095.

[56] N.M. Glykos, Carma: a molecular dynamics analysis program, J. Comput. Chem. 27 (2006) 1765–1768.

[57] J. Li, V.N. Uversky, A.L. Fink, Effect of familial Parkinson's disease point mutations A30P and A53T on the structural properties, aggregation, and fibrillation of human α-synuclein, Biochemistry 40 (2001) 11604–11613.

[58] D. Balesh, Z. Ramjan, W.B. Floriano, Unfolded annealing molecular dynamics conformers for wild-type and disease-associated variants of alpha-synuclein show no propensity for beta-sheetformation, J. Biophys. Chem. 02 (2011) 124–134.

[59] F.A. Buratti, N. Boeffinger, H.A. Garro, J.S. Flores, F.J. Hita, P.C. Gonçalves, F.D. R. Copello, L. Lizarraga, G. Rossetti, P. Carloni, M. Zweckstetter, T.F. Outeiro, S. Eimer, C. Griesinger, C.O. Fernández, Aromaticity at position 39 in α-synuclein: A modulator of amyloid fibril assembly and membrane-bound conformations, Protein Sci. 31 (2022) e4360.

[60] L.E. Wilkinson-White, S.B. Easterbrook-Smith, A dye-binding assay for measurement of the binding of cu(II) to proteins, J. Inorg. Biochem. 102 (2008) 1831–1838.

[61] F.R. Dutra, C.D.S. Silva, R. Custodio, On the accuracy of the direct method to calculate pKa from electronic structure calculations, J. Phys. Chem. A 125 (2021) 65–73.